Available online at www.sciencedirect.com
ScienceDirect
Planetary and Space Science 56 (2008) 941–946
Planetary and Space Science
www.elsevier.com/locate/pss

Density cavity observed over a strong lunar crustal magnetic anomaly in the solar wind: A mini-magnetosphere?

J.S. Halekas*, G.T. Delory, D.A. Brain, R.P. Lin, D.L. Mitchell

Space Sciences Laboratory, 7 Gauss Way, University of California, Berkeley, CA 94720, USA

Received 23 October 2007; received in revised form 17 December 2007; accepted 18 January 2008
Available online 30 January 2008

Abstract

We present observations of what may be the inner region of a lunar mini-magnetosphere. If so, these likely represent the first such observations. Previous studies of solar wind interaction with lunar crustal magnetic fields found increased particle fluxes associated with magnetic amplifications, suggesting a shock/sheath region. The central density cavity expected in the inner mini-magnetosphere (if analogous to other planetary magnetospheres) has proven elusive. We now present Lunar Prospector fly-throughs of a density cavity near a strong crustal magnetic source in the solar wind, and compare these unique observations with typical orbits in the solar wind and wake. We observed the density cavity on two consecutive orbits on July 14, 1999 with optimal viewing geometry, downstream from one of the strongest lunar crustal sources (an anomaly centered at ~235E, 20S), during very unusual solar wind conditions. We found no other similar features in the solar wind in ~7 months of low-altitude orbits, suggesting that fully formed lunar mini-magnetospheres are rare and/or difficult to observe from orbit.

Keywords: Moon; Mini-magnetosphere; Density cavity; Lunar prospector

1. Introduction

The Moon has neither a global magnetic field nor a significant atmosphere, and to first order behaves as a solid obstacle. In the solar wind, the Moon blocks and absorbs the supersonic flowing plasma, while allowing magnetic fields to pass through with only minor modifications from diamagnetic current systems around the wake boundary, which produce a moderate magnetic amplification in the wake cavity and a reduction in the magnetic field in the surrounding expansion region (Colburn et al., 1971; Halekas et al., 2005).

Extensive (albeit weak) lunar crustal magnetic fields (see, e.g., Hood et al., 2001) perturb this basic picture. External to the expansion region, many spacecrafts have observed magnetic enhancements, clearly associated with crustal magnetic sources (but too strong for uncompressed crustal fields), which have been variously termed lunar external magnetic enhancements (LEMEs), limb shocks, and limb compressions (Ness et al., 1968; Colburn et al., 1971; Russell and Lichtenstein, 1975; Lin et al., 1998; Halekas et al., 2006, 2007). These magnetic amplifications form near crustal magnetic fields large and strong enough to slow or stop the solar wind plasma, creating magnetosonic compressional waves which, for a sufficiently strong interaction, may steepen to form a shock reaching upstream of the source. Early investigations found these features only near the limb, but Lunar Prospector (LP) observed LEMEs at spacecraft altitudes as high as ~100 km well upstream ($>45^\circ$) from the limb (Lin et al., 1998). Given the Mach cone angle for magnetosonic waves in the solar wind ($<\sim 20^\circ$) and the resulting inability of compressional waves to reach the spacecraft at these times, these observations strongly argue for the presence of a shock extending upstream of the source.

Simulations leave it uncertain as to whether we should expect to find fully formed mini-magnetospheres associated with lunar crustal magnetic sources, given the weakness of the magnetic fields and the small size of the effective

*Corresponding author. Tel.: +1 510 6434310; fax: +1 510 6438302.
E-mail address: jazzman@ssl.berkeley.edu (J.S. Halekas).

0032-0633/$ - see front matter © 2008 Elsevier Ltd. All rights reserved.
doi:10.1016/j.pss.2008.01.008

obstacles to the solar wind flow. Some simulations of solar wind interaction with dipolar features would predict a whistler wake or magnetosonic wake rather than a magnetosphere for the lunar case (Omidi et al., 2002), but other simulations show that the non-dipolar nature of lunar crustal magnetic sources might increase the efficiency of the interaction, perhaps producing a magnetosphere (Harnett and Winglee, 2003). In any case, the ability of crustal fields to stand off the solar wind, and the apparent sporadic presence of bow shocks, suggests that mini-magnetospheres could potentially form over the strongest lunar crustal sources. One observational study, at least, has claimed the positive identification of a mini-magnetosphere, based on magnetic field data over the Reiner Gamma anomaly in the solar wind (Kurata et al., 2005).

Most previous investigations of LEMEs have focused on the magnetic field amplifications. Those studies that considered plasma data (Siscoe et al., 1969; Lin et al., 1998; Halekas et al., 2007) all found increases in charged particle fluxes associated with LEMEs. If lunar mini-magnetospheres exist and are morphologically similar to other planetary magnetospheres, this suggests that observations to date may have only revealed the structure of the shock and possibly sheath regions (where plasma density should increase), while missing the inner magnetosphere (where density should decrease). Lunar mini-magnetospheres may completely lack central density cavities, or density cavities may merely prove rare and/or difficult to observe. If central density cavities do not exist, the term "mini-magnetosphere" might, in our opinion, prove something of a misnomer.

After an exhaustive search of the entire LP data set, we now present observations which show the presence of a density cavity just downstream from a strong crustal magnetic anomaly in the solar wind (on two consecutive orbits), potentially revealing for the first time the structure of the inner regions of a lunar mini-magnetosphere. We preface these unique observations by first discussing more typical magnetic field and plasma observations over the same crustal source in the lunar plasma wake and in the solar wind, in order to compare and contrast these typical observations with the newly discovered mini-magnetospheric observations.

2. Lunar prospector electron and magnetic field data

LP had two instruments relevant to lunar mini-magnetospheres—a magnetometer (MAG), and an Electron Reflectometer (ER) (Lin et al., 1998). The MAG was a tri-axial fluxgate magnetometer, which measured the vector magnetic field at 9 Hz. The ER was a top-hat electrostatic analyzer, which measured electron fluxes from tens of eV to tens of keV, in two different modes. The ER collected 3-d data (covering all energies and angles) every 80 s, and pitch angle sorted data (sorted into pitch angle bins using the instantaneous magnetic field measurement onboard the spacecraft) for selected energies at higher time resolutions, at best every 2.5 s (at 142 and 337 eV). The LP spacecraft orbited at ~1.6 km/s, so these time resolutions correspond to lateral resolutions of ~130 and ~4 km, respectively, both adequate to capture the interaction with most significant crustal anomalies, though with poor resolution in the case of the 3-d measurements. In this paper, we show both low and high time resolution data (both summed over all angles), allowing a determination of both the energy dependence of the electron fluxes and their spatial variation at the highest possible resolution.

In addition, we calculate electron moments by fitting suprathermal electron distributions to Kappa distributions (essentially Maxwellian distributions with high-energy power-law tails, generally more representative of solar wind spectra than a single Maxwellian), as described by Halekas et al. (2005). We can only perform this calculation using the full-energy spectrum, limiting moments to the lower time resolution of the 3-d data. Because of the limited low-energy coverage, the moments thereby calculated cannot always fully capture the thermal distribution of the electrons, so we choose to divide by the average moments in the solar wind in order to obtain normalized quantities for both temperature and density, and focus on relative magnitudes rather than absolute.

3. Observations over strong crustal fields in the lunar wake

We first consider typical observations over a strong crustal source in the lunar wake, where the lunar surface and crustal fields are shielded from the incidence of the solar wind. Fig. 1 shows almost half an orbit on May 21, 1999 over the Crisium Antipode (CA) anomaly, one of the strongest lunar crustal magnetic field sources (Hood et al., 2001), as LP passes through the lunar wake. The CA anomaly is roughly centered at 235E, 20S, and extends over ~10° in longitude and ~20° in latitude, with a complex non-dipolar morphology. We can easily identify the CA anomaly by the large peak in magnetic field magnitude, and rotations in the field direction. The full rotations in the magnetic field are consistent with direct measurements of unperturbed crustal fields, as expected in this near-vacuum environment.

The overall density decrease and moderate temperature increase in the central wake represent characteristic features observed on most orbits through the lunar wake, which have been successfully modeled in terms of non-Maxwellian solar wind plasma refilling the wake cavity (see Halekas et al., 2005). On top of the wake density depletion, the electron density drops at least another order of magnitude compared to the local plasma in the near vicinity of the CA anomaly. The high time resolution data suggests that the density drop may even exceed an order of magnitude over a smaller region.

Unfortunately, at present we cannot correct electron fluxes and moments for the effects of spacecraft charging in shadow. Theoretical calculations and initial data analyses suggest spacecraft charging in the wake to negative

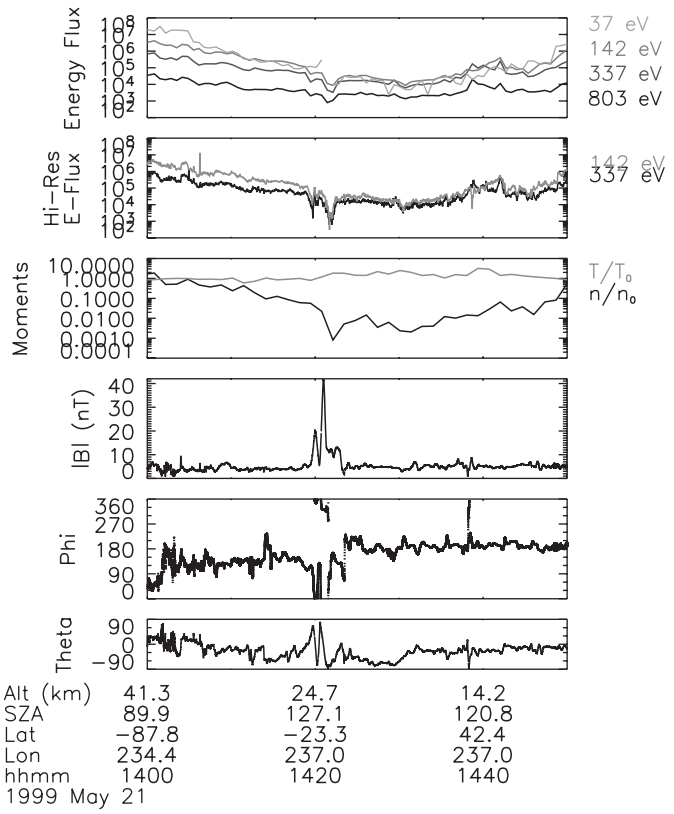

Fig. 1. An orbit over the CA (Crisium Antipode) magnetic anomaly in the lunar wake, showing differential energy flux in eV/(cm^2 s ster eV) at low and high time resolution, fitted moments (normalized), and magnetic field magnitude and angles (in Selenocentric Solar Ecliptic coordinates). The orbital altitude, solar zenith angle (SZA), planetary longitude and latitude, and UT time are listed at the bottom of the figure.

potentials <100 V (Halekas et al., 2005). Negative spacecraft charging will affect electron measurements by slowing incoming electrons and excluding the lowest-energy part of the distribution, so we must consider these wake electron measurements only lower bounds. However, the inferred electron temperature does not change markedly in the plasma void, which ensures the approximate validity of at least the relative flux and density drop shown here.

We searched through all low-altitude LP orbits (~7 months of data) in the lunar wake, and found over a thousand such examples of plasma voids, most clearly associated with crustal magnetic sources. Initial modeling of the Reiner Gamma anomaly (utilizing an array of dipoles corresponding in extent to the Reiner Gamma albedo marking and fitting to LP MAG data) and particle tracing in modeled fields indicates that plasma voids correspond closely with regions with closed magnetic field geometry. Plasma on these field lines has presumably hit the surface, recombined, or otherwise been lost shortly after lunar sunset, before LP encountered these regions. Any source processes must operate more slowly than loss processes, leading to the nearly complete plasma voids associated with many crustal sources. These voids closely resemble the much larger plasma voids observed over crustal magnetic anomalies in the Martian magnetotail (Brain et al., 2007), and the physical processes responsible for their formation and evolution are likely also similar. These observations show that, when shielded from the solar wind, lunar crustal magnetic anomalies can sustain density cavities.

4. Observations over strong crustal fields in the solar wind

We continue by considering typical observations over the same CA magnetic anomaly, but now located in the solar wind rather than the near-vacuum of the wake. Fig. 2 shows a portion of an orbit on April 10, 1999 at nearly the same planetary longitude as Fig. 1, but on the dayside, well upstream from the limb.

All of the quantities plotted in Fig. 2 correspond directly to those in Fig. 1, with one exception. In sunlight, we can now successfully correct the low time resolution 3-d data for the effects of spacecraft charging. To achieve this correction, we used data from the magnetotail, when the

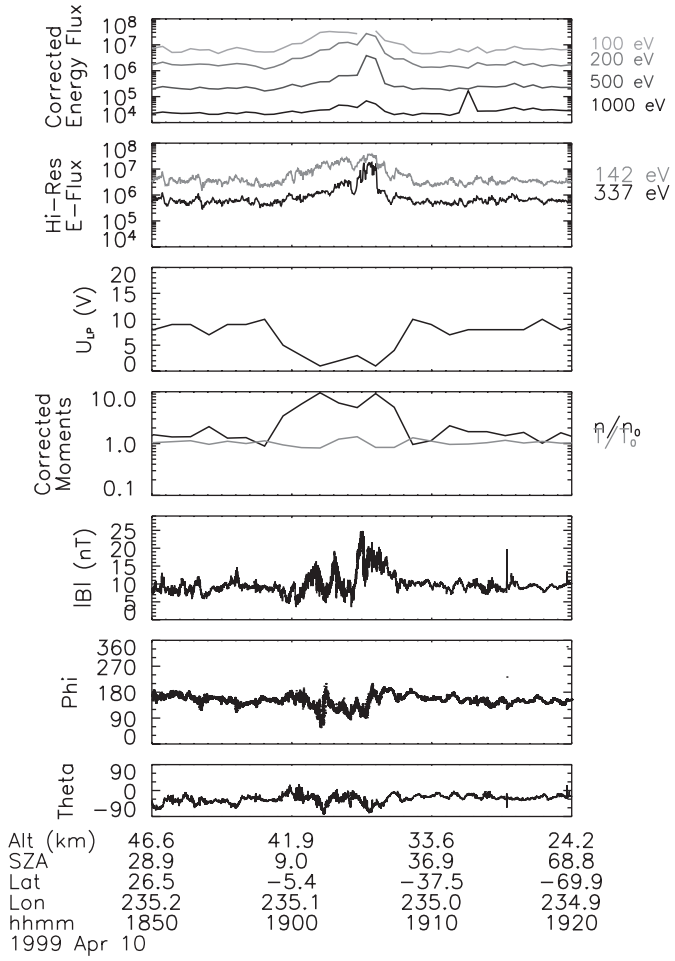

Fig. 2. An orbit over the CA magnetic anomaly in the solar wind, showing differential energy flux at low and high time resolution, spacecraft potential, moments, and magnetic field.

energy sweep of the ER at times extended down to a few eV, to measure both the full incident electron distribution and the photoelectron distribution attracted back to the positively charged spacecraft. By identifying the break in the electron energy spectrum between these two distributions, we determined the spacecraft potential as a function of incident electron current, and successfully fit this to a simple exponential function. With this function in hand, we can now approximately correct for spacecraft potential for all LP ER 3-d data obtained in sunlight, by fitting to the electron distribution to determine the incident current, and employing an iterative method similar to that described by Scudder et al. (2000). Ions also represent a significant current source in the solar wind, but one can easily determine that their effect on the equilibrium spacecraft potential remains minimal in most regimes (Scudder et al., 2000). We can therefore use the same methodology to determine the spacecraft potential and corrected electron fluxes and moments (shown in Fig. 2) in the solar wind. We can only do this for the low time resolution 3-d data, since we need the full-electron energy spectrum.

In the solar wind, unlike in the wake, we can no longer expect vacuum superposition of fields. Indeed, we observe a qualitatively different magnetic signature. First, we find a weaker magnetic field; however, the higher spacecraft altitude and slightly different planetary longitude make it difficult to make direct quantitative comparisons. More importantly, though, we observe a very different character in the magnetic field polarity. In contrast to the full rotations observed in the wake, we find only a moderate rotation from the unperturbed solar wind direction. This suggests that the magnetic field we observe may consist primarily of compressed solar wind magnetic field, rather than a direct measurement of the crustal magnetic field. This is consistent with magnetic field draping and pileup over the magnetic obstacle, as suggested by previous observations (Lin et al., 1998; Halekas et al., 2006).

In addition, rather than the density depletion observed in the wake, we now find a density enhancement roughly coincident with the magnetic field amplification. This is consistent with an observation of a shock, as suggested by the magnetic field data. We find a similar morphology to that observed here for most orbits over strong crustal magnetic fields in the solar wind (Halekas et al., 2006, 2007). Interestingly, on this orbit the electron temperature remains relatively constant. Previous observations suggest heating of electrons near LEMEs (Lin et al., 1998), but some evidence suggests that the electron heating correlates more strongly with upstream magnetic turbulence and whistler wave activity than with the shocks themselves (Halekas et al., 2007). In any case, if these observations represent mini-magnetospheres with a similar morphology to other planetary magnetospheres, we have clearly traversed only the outer regions thus far, without reaching the inner magnetosphere.

5. Direct observations of a mini-magnetosphere

5.1. Observations

We conducted an exhaustive search of all low-altitude LP electron data to locate density cavities (which might represent the inner regions of mini-magnetospheres) associated with crustal magnetic fields in the solar wind. Fig. 3 shows the result of this search. Out of ~7 months of low-altitude data, we found only two examples of clear density dropouts in the 3-d electron data, on two consecutive orbits on July 14, 1999 near the CA anomaly. These two orbits lie almost 10° away from those shown in Figs. 1 and 2, at 243–244 E, actually slightly downstream (with respect to the solar wind flow) from the CA anomaly. The LP orbit at this time lies close to the dawn-dusk plane, and thus the spacecraft remains sunlit over the entire orbit. Wind SWE (Ogilvie et al., 1995) observations upstream from the Moon during this orbit show very nearly anti-sunward solar wind flow, and these potential mini-magnetospheric observations lie 7–8° upstream from the limb and ~30 km above the surface, therefore inarguably in the solar wind even taking aberration into account.

At the closest approach to the CA anomaly (at 15:43 and 17:33), on both orbits, we observe a density dropout of over an order of magnitude associated with a magnetic enhancement. The spacecraft potential increases significantly in both of these density cavities, where the incident electron current cannot balance as much of the escaping photoelectron current. We found accurate corrections for this spacecraft potential crucial in determining the true variation of the electron fluxes, especially at the lowest energies.

The magnetic field surprisingly shows very little rotation in these possible mini-magnetospheres, remaining more consistent with draped solar wind magnetic fields than with direct measurements of crustal fields. Wind also observes the large rotations in the phi component at approximately 16:10, 16:40, and 17:45 upstream, so they have no relation to the interaction with the crustal fields. We find it somewhat surprising that the density cavities would not correspond to measurements of crustal magnetic fields. These observations may actually represent the magnetotail region downstream of the magnetic obstacle, rather than the inner magnetosphere; however, even in this case one would still expect strongly draped magnetic fields which would not correspond so closely in polarity to the solar wind field.

5.2. Context

At no other time during the LP low-altitude extended mission did we see similar density cavities in the solar wind, demonstrating the uniqueness of these observations. We also investigated the high time resolution data to find more localized flux dropouts, since though these would not necessarily indicate density cavities (because of the limited

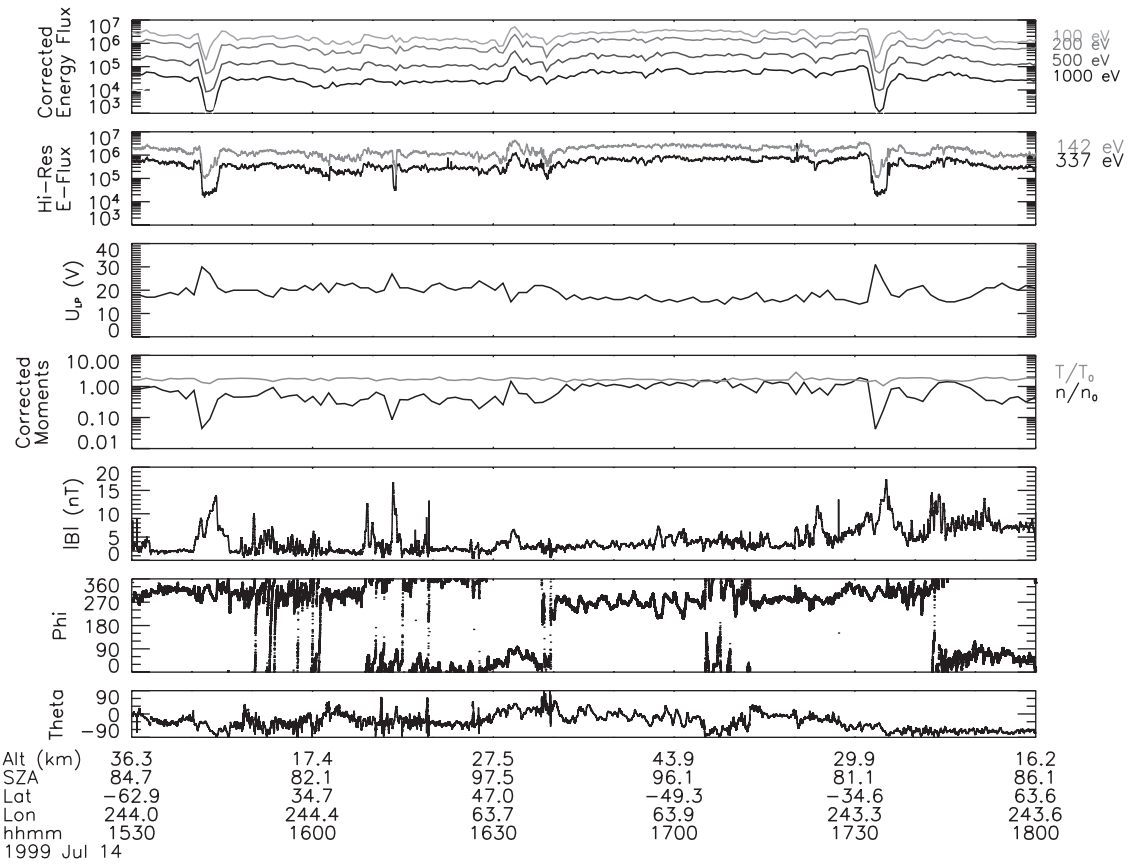

Fig. 3. Two orbits just downstream from the CA magnetic anomaly in the solar wind, showing differential energy flux at low and high time resolution, spacecraft potential, moments, and magnetic field.

energy coverage), they might give us an idea of whether more localized density cavities might exist. We found only a few other order of magnitude drops in flux in the high time resolution data in the solar wind, all of which occurred on either this same day, the following day or on February 10, 1999. One such localized dropout occurred during the same time period shown in Fig. 3, at 16:15, over a small crustal anomaly well to the north of CA (at 245E, 80N). If density dropouts commonly existed over such small anomalies as this in the solar wind, we should observe them quite frequently; indeed, we should see thousands of plasma voids, as we do in the wake. The fact that we do not suggests some special property of the orbits shown in Fig. 3, either in terms of viewing geometry or solar wind conditions.

The viewing geometry on these orbits is undeniably fortuitous, allowing us to view the solar wind interaction with a very strong crustal magnetic source near the terminator, where the normal pressure of the solar wind minimizes, allowing the interaction to extend to higher altitudes. However, we have many LP observations in similar orbits, many near equally strong crustal magnetic sources, at equally low altitudes, and have never observed any other density cavities on these orbits. Therefore, while the viewing geometry certainly helps, it alone likely cannot explain these observations.

Instead, it appears likely that unique solar wind conditions may explain the observations presented here. We determined the upstream solar wind conditions using wind SWE and MFI data (Ogilvie et al., 1995; Lepping et al., 1995), and shifted them in time appropriately according to the solar wind velocity and the 3-d separation between wind and LP, as described by Halekas et al., (2005). We found rather peculiar average solar wind conditions (as compared to the rest of the LP mission) during the period shown in Fig. 3, including a very high solar wind density (15.8 cm^{-3}), low solar wind proton temperature (1.11 eV), low solar wind velocity (303 km/s), low solar wind magnetic field (2.36 nT) and high solar wind Alfven and magnetosonic Mach numbers (23.4, 9.0). All of these values lie on the extreme wing of their respective distributions as compared to observations during the rest of the LP mission (96th percentile for velocity, 98th for temperature, 92nd for density, 99th for magnetic field, 99th for M_A, and 98th for M_{MS}—where we define percentile as the percentage of observations lying below a high value or above a low value), making this a very unusual solar wind. It seems likely that these solar wind conditions must contribute to an increased likelihood of observing the central mini-magnetospheric density cavity (or an increased likelihood of its existence).

However, though the unique solar wind conditions almost certainly contribute to observation of density cavities on these particular orbits, the physical mechanism remains unclear. What little we know about LEMEs would not necessarily lead us to believe that these conditions would prove particularly fortuitous for observing the inner mini-magnetosphere. Indeed, high Mach number should actually compress the interaction region, with previous observations indicating that a high Mach number makes the observation of an LEME less likely (Halekas et al., 2006). Previous observations do show that low solar wind proton temperature increases the likelihood of observing an LEME, but solar wind density, magnetic field and velocity do not obviously affect the interaction (Halekas et al., 2006).

Given expectations from theory and simulations (Omidi et al., 2002), one would expect that a reduction in the ion inertial length would most significantly increase the chance of observing the central density cavity, since the ion inertial length sets the scale size of various interaction regions. In accordance with this, we do find an ion inertial length of 57 km, only moderately smaller than the average value of ~97 km, but still a 92nd percentile observation (as defined above) because of the relatively narrow distribution for ion inertial length. One might not expect a 40% reduction in this parameter to have such a huge effect, but perhaps given the other unusual solar wind conditions, this may provide at least part of the answer to the puzzle.

6. Implications and conclusions

We have presented what may be the first observations of the inner regions of a lunar mini-magnetosphere; however, many questions remain. We do not yet understand why observations of density cavities over strong crustal anomalies have proven so rare. In the wake, away from the bombardment of the solar wind, plasma voids over strong crustal fields have proven quite common. However, in the solar wind, we instead usually observe density enhancements, consistent with location in a shock or sheath region. Though we have finally observed density cavities, which may prove to represent the inner regions of a mini-magnetosphere, we do not understand the magnetic field morphology, nor do we know why we could observe them on the two orbits presented in this paper (and only those two orbits). It seems likely that the combination of a fortuitous orbital geometry near one of the strongest crustal magnetic sources, and very unique solar wind conditions, can at least partially explain this. However, the difficulty of observing these features suggests that fully formed mini-magnetospheres may prove quite rare and/or difficult to observe. In any case, many low-altitude observations with a much more complete plasma package than that afforded by LP will be required before we can fully understand the unique solar wind interaction with lunar crustal magnetic fields.

Acknowledgements

We thank the wind MFI and SWE teams and the Lunar Prospector MAG/ER team for data used in this investigation. We thank two reviewers for helpful and constructive comments, which strengthened this manuscript.

References

Brain, D.A., Lillis, R.J., Mitchell, D.L., Halekas, J.S., Lin, R.P., 2007. Electron pitch angle distributions as indicators of magnetic field topology near mars. J. Geophys. Res. 112, A09201.

Colburn, D.S., Mihalov, J.D., Sonett, C.P., 1971. Magnetic observations of the lunar cavity. J. Geophys. Res. 76, 2940–2957.

Halekas, J.S., Bale, S.D., Mitchell, D.L., Lin, R.P., 2005. Electrons and magnetic fields in the lunar plasma wake. J. Geophys. Res. 110, A07222.

Halekas, J.S., Brain, D.A., Mitchell, D.L., Lin, R.P., Harrison, L., 2006. On the occurrence of magnetic enhancements caused by solar wind interaction with lunar crustal fields. Geophys. Res. Lett. 33, L01201.

Halekas, J.S., Brain, D.A., Lin, R.P., Mitchell, D.L., 2007. Solar wind interaction with lunar crustal magnetic anomalies. J. Adv. Space Res. (in press).

Harnett, E.M., Winglee, R., 2003. 2.5-D simulations of the solar wind interacting with multiple dipoles on the surface of the Moon. J. Geophys. Res. 109, 1088.

Hood, L.L., Zakharian, A., Halekas, J., Mitchell, D.L., Lin, R.P., Acuña, M.H., Binder, A.B., 2001. Initial mapping and interpretation of lunar crustal magnetic anomalies using Lunar Prospector magnetometer data. J. Geophys. Res. 106, 27,825–27,840.

Kurata, M., Tsunakawa, H., Saito, Y., Shibuya, H., Matsushima, M., Shimizu, H., 2005. Mini-magnetosphere over the Reiner gamma magnetic anomaly region on the moon. Geophys. Res. Lett. 32, L24205.

Lepping, R.P., et al., 1995. The WIND magnetic field investigation. Space Sci. Rev. 71, 207–229.

Lin, R.P., Mitchell, D.L., Curtis, D.W., et al., 1998. Lunar surface magnetic fields and their interaction with the solar wind: results from lunar prospector. Science 281, 1480–1484.

Ness, N.F., Behannon, K.W., Taylor, H.E., Whang, Y.C., 1968. Perturbations of the interplanetary magnetic field by the lunar wake. J. Geophys. Res. 73, 3421–3440.

Ogilvie, K.W., et al., 1995. SWE, a comprehensive plasma instrument for the WIND spacecraft. Space Sci. Rev. 71, 55–77.

Omidi, N., Blanco-Cano, X., Russell, C.T., Karimabadi, H., Acuña, M., 2002. Hybrid simulations of solar wind interaction with magnetized asteroids: general characteristics. J. Geophys. Res. 107, 1487.

Russell, C.T., Lichtenstein, B.R., 1975. On the source of lunar limb compressions. J. Geophys. Res. 80, 4700–4711.

Scudder, J.D., Cao, X., Mozer, F.S., 2000. Photoemission current-spacecraft voltage relation: key to routine, quantitative low-energy plasma measurements. J. Geophys. Res. 105, 21,281–21,294.

Siscoe, G.L., Lyon, E.F., Binsack, J.H., Bridge, H.S., 1969. Experimental evidence for a detached lunar compression wave. J. Geophys. Res. 74, 59–69.